Using 129Xe NMR to Probe the Structure of Ionic Liquids

ARTICLE *in* JOURNAL OF PHYSICAL CHEMISTRY LETTERS · AUGUST 2013

Impact Factor: 7.46 · DOI: 10.1021/jz401279u

THE JOURNAL OF PHYSICAL CHEMISTRY Letters

Letter

pubs.acs.org/JPCL

Using ^{129}Xe NMR to Probe the Structure of Ionic Liquids

Pedro Morgado,[†] Karina Shimizu,[†] José M. S. S. Esperança,[‡] Patrícia M. Reis,[‡] Luís P. N. Rebelo,[‡] José N. Canongia Lopes,*[,†,‡] and Eduardo J. M. Filipe*[,†]

[†]Centro de Química Estrutural, Instituto Superior Técnico, Universidade Técnica de Lisboa, 1049-001 Lisboa, Portugal

[‡]Instituto de Tecnologia Química e Biológica (www.itqb.unl.pt), Universidade Nova de Lisboa, 2750-154 Oeiras, Portugal

Supporting Information

ABSTRACT: The mesoscopic structure of 30 distinct ionic liquids was probed by ^{129}Xe NMR spectroscopy. The interpretation of the experimental data was complemented using molecular dynamics results. The results clearly show that xenon can effectively probe the various environments characteristic of different ionic liquids (ILs) and is thus able to distinguish between distinct ionic liquid families, including different types of interactions with diverse types of anion/polar networks. A finer analysis of the NMR data also confirmed that the xenon probes can also provide information on how the complex structure of an IL evolves along a homologous series.

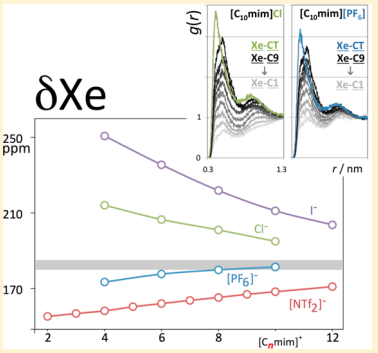

SECTION: Liquids; Chemical and Dynamical Processes in Solution

Ionic liquids (ILs) are fluids characterized by an intricate balance between electrostatic, van der Waals, and hydrogen-bond interactions. Such a balance hinders the formation of long-range crystalline structures around room temperature but nevertheless imposes a sort of mesoscopic ordering in the fluid phase. As such, ILs are recognized as nanosegregated fluids, composed of a polar network that is permeated by more or less extensive nonpolar domains. This feature of ILs has major consequences for their macroscopic properties, namely, their solvation toward different types of molecular compounds.

The structure of ILs has been analyzed using different techniques, from X-ray diffraction experiments[1] to molecular dynamics (MD) modeling.[2,3] Calorimetry, viscosimetry, diffusivity, or electrical conductivity data as well as numerous spectroscopic experiments have also been used to highlight the presence of nanoscale segregation that, logically, has an impact on the static and dynamic properties of the systems, namely, on the trends observed when the length of the alkyl side chains of the ions is increased.[4−17] Other examples include fluorescence studies[18] that revealed red shifts characteristic of organized media with long-lived structures or the use of solvatochromic probes to study different environments in the IL media.[19]

^{129}Xe NMR spectroscopy has been widely used to provide information on the structural and dynamic properties of a range of systems including simple liquids, isotropic and anisotropic solutions, biological systems, and various solid materials.[20−24] New applications, such as ^{129}Xe NMR imagery, are being developed.[25] Given its chemical quasi-inertness, high natural abundance, −1/2 nuclear spin, and large and highly polarizable electron cloud, ^{129}Xe is a very effective NMR probe, with a chemical shift range exceeding 200 ppm.[26]

Molecular probes can often present disadvantages as many of the observed effects cannot be separated from those caused by the presence of a bulky probe. In the case of xenon, however, it has been shown[27] that it can be modeled as a simple sphere, using potential parameters similar to those used to describe the *n*-alkanes family. Xenon can thus be viewed as the smallest alkane that , when dissolved in a liquid, will produce a minimal perturbation.

We recently published an extensive body of data of ^{129}Xe chemical shifts, δXe, in liquid alkanes (linear, cyclic, and branched) measured as a function of temperature.[28] We showed that the δXe in all of these solvents is determined by the density, nature, and organization of the chemical groups within xenon's first coordination sphere. Moreover, by examining spectra as a function of temperature, we demonstrated how important it is to compare δXe values at similar thermodynamic conditions, defined, for example, at the same reduced temperature or the same density of the solvent. At 298 K, δXe values from *n*-butane to *n*-hexadecane vary from 140 to 240 ppm; at a common reduced temperature (T_r) of 0.4, the range of δXe in alkanes falls to less than 4 ppm, depending on the fraction of CH_3 groups in the solvent molecule. Perfluoroalkanes, on the other hand, exhibit weak dispersion forces relative to their hydrogenated counterparts. Accordingly, at 298 K, their δXe values are much smaller, ranging from 65 to 100 ppm; it will also fall to a few ppm range if a common reduced temperature is considered.

Received: June 20, 2013
Accepted: July 31, 2013

   dx.doi.org/10.1021/jz401279u | *J. Phys. Chem. Lett.* 2013, 4, 2758−2762

Building on this previously accumulated knowledge, we demonstrate in this Letter that ^{129}Xe NMR spectroscopy can be advantageously used to obtain molecular-level evidence of the nanostructuring of ILs. The results below show that xenon is able to clearly distinguish between different families of ILs and, more importantly, that it can also provide information on how the complex mesoscopic organization of the liquid progresses as the alkyl side-chain length of the ions increases.

In a very recent work,[29] Castiglioni et al. reported for the first time ^{129}Xe NMR results for a number of ILs. Their work deals with 1-ethyl-3-methylimidazolium or 1-butyl-3-methylimidazolium cations combined with 10 different anions and demonstrates how xenon is able to differentiate between anions of diverse nature. The authors proposed that xenon atoms occupy cage-like cavities similar to those found in the IL's crystalline phases and proposed a qualitative correlation between the observed δXe trends and such cage dimensions; larger and smaller cavities would produce smaller and larger δXe values, respectively. However, the proposed explanation does not consider the influence of the polarizability of the atoms that compose the different anions and fails to explain, for instance, the trends found among halide-based ILs.

From an experimental point of view, the simplicity of the technique is one of its main assets; gaseous xenon can be bubbled directly through the purified IL sample already inside of the NMR tube, and spectra can be immediately recorded (cf. the Supporting Information (SI)). The low solubility of xenon in the studied ILs (estimated to be less than 1.5% mole fraction in $[C_6mim][Ntf_2]$ at 298 K[30]) is sufficient to obtain accurate spectra while preventing solute−solute interactions. All spectra were thus obtained at atmospheric pressure, thus avoiding the need to assess the effect of pressure in the δXe values. As for the temperature effect, as previously explained, δXe values in different solvents should be compared at the same thermodynamic state, for example, at the same reduced temperature. In the case of ILs, however, it is known that their estimated critical temperatures are very high (>1000 K).[31] Consequently, at room temperature, ILs are practically all at the same reduced temperature (~0.25), and this fact explains the small temperature dependence experimentally observed (cf. the SI).

The δXe values at 298.17 K of ^{129}Xe dissolved in four IL homologous series based on 1-alkyl-3-methyl-imidazolium cations, $[C_nmim]^+$, combined with different anions are represented in Figure 1 as a function of the alkyl chain length, n. Results for a few other isolated ILs are also included in the figure. It must be stressed that the NMR measurements were conducted as a function of temperature. The full collection of data is given as SI.

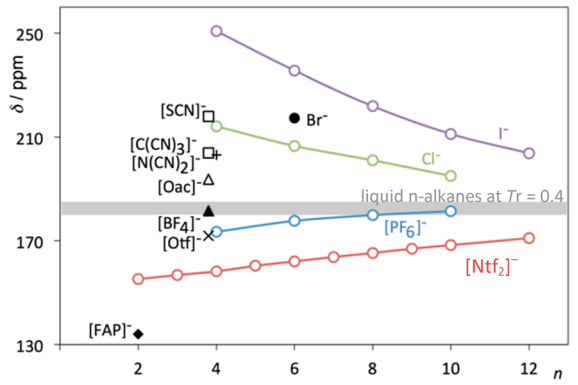

Figure 1. ^{129}Xe chemical shifts, δ, as a function of the alkyl chain length, n, in different 1-alkyl-3-methylimidazolium-based ILs. $[Oac]^-$ = acetate, $[Otf]^-$ = triflate, $[FAP]^-$ = tris(perfluoroethyl)-trifluorophosphate.

Among the four homologous series, the highest ^{129}Xe solvent shifts are produced by the iodide series, followed by chloride (δXe in $[C_6mim]Br$ falls between the corresponding $[C_6mim]I$ and $[C_6mim]Cl$ values). In both cases, δXe decreases with increasing alkyl side-chain lengths, n. In the series based on $[PF_6]^-$ and bis(trifluoromethylsulfonyl)imide, $[Ntf_2]^-$, ions, the behavior is different, starting with smaller δXe values that increase with n. All ILs with fluorinated anions display δXe values below 185 ppm. It is clear that ILs with highly fluorinated anions display the smallest δXe values, as could be expected from our previous results of perfluoroalkanes.[28] In the case of the iodide and chloride series, the presence of the heavier atoms enhances the dispersive interactions with xenon and is responsible for higher δXe results, again in agreement with previous observations.[32]

Also represented in Figure 1 is the range of δXe values observed when the solvent is a dense liquid alkane at a reduced temperature of 0.4 (e.g., hexadecane at 298.15 K). All IL homologous series seem to come near to this range as the length of the corresponding alkyl side chains increases, and this suggests the progressive solvation of xenon in alkyl-like regions within the IL. This explains the different trends observed for the different series: (i) for small n values, the observed δXe values are dominated by interactions with the polar regions of the IL where the intrinsic polarizability of the different anions produce different δXe values; (ii) for longer alkyl chain lengths, the interactions with the nonpolar regions become progressively more important, and the alkane limit is gradually approached.

In order to further discuss the possible location of the xenon atoms within the IL, we have used MD simulations. Fifteen IL systems were selected, containing five types of cations (1-alkyl-3-methylimidazolium ions with n = 2, 6, 10, 14, and 18) combined with three types of anions (chloride, hexafluorophosphate, and bis(trifluoromethylsulfonyl)imide). To avoid solute−solute interactions, each simulation box contained a single xenon atom "diluted" in IL solvents occupying more than 30 nm^3. To improve the poor statistics associated with the solute−solvent distribution functions, the simulation trajectories were evaluated at moderate temperatures over consecutive periods (at least three) of more than 6 ns each. Furthermore, two independent simulations were always performed and compared for each system in order to detect possible ergodicity issues.

Some of the most representative results, the solute−solvent radial distribution functions (RDFs) between xenon and selected interaction centers in the cations, are presented in Figure 2. Other RDFs that show the nanostructuring of the IL (solvent−solvent RDFs) or illustrate the different xenon−anion interactions are given as SI.

The three panels of Figure 2a show the distribution of xenon in the vicinity of the polar network (around the imidazolium ring carbon atom at position 2, CR, cf. Scheme 1) as the alkyl chain of the cation is increased and the nature of the anion is changed. The RDFs of the three $[C_2mim]$-based ILs (darker colors in each panel) can be thought of as the baseline behavior for each type of IL; the nonpolar regions are practically nonexistent in this case, which means that the xenon atoms must never stay far from the polar network of the IL. The first

dx.doi.org/10.1021/jz401279u | J. Phys. Chem. Lett. 2013, 4, 2758−2762

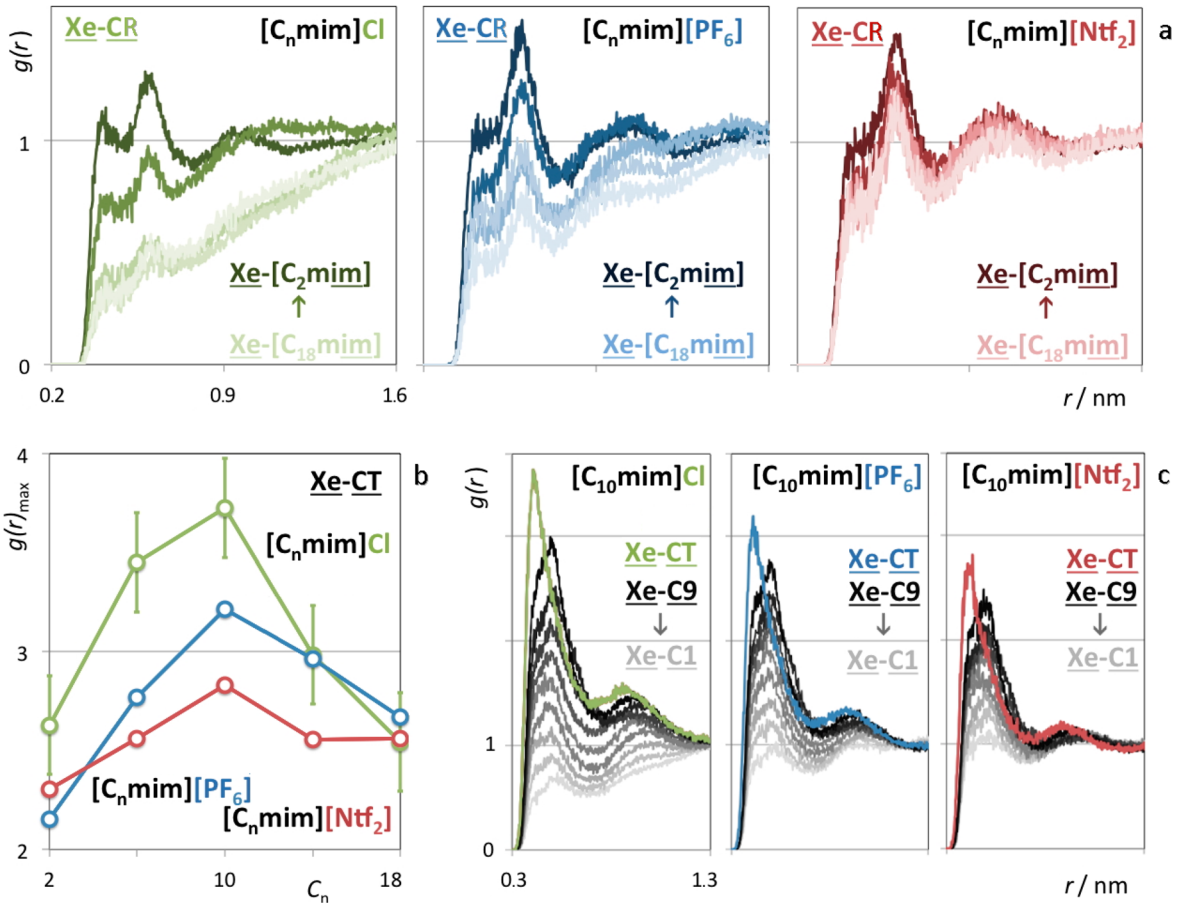

Figure 2. Xe IL radial distribution functions (RDFs) obtained by MD simulation. (a) Xe-imidazolium ring RDFs (Xe-CR); (b,c) Xe-alkyl side chain RDFs. Compare with the Scheme 1 nomenclature.

Scheme 1. Nomenclature of the 1-Alkyl-3-methylimidazolium Cation

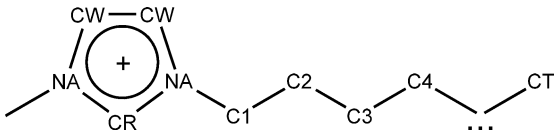

peaks of the RDF (a double peak in the case of the chloride IL that changes into a shoulder peak in the case of the $[PF_6]^-$ and $[Ntf_2]^-$ ILs) do not reflect any strong interaction between the xenon solute and the charged parts of the IL as the RDF intensities are never much larger than unity. Interestingly, the relatively small chloride anion (that interacts very strongly with the CR atom) allows for the presence of the xenon atom in the CR vicinity because it cannot occupy the entire volume surrounding CR. In the case of the $[PF_6]^-$ and $[Ntf_2]^-$ anions (larger, polycentered, and flexible), the xenon atoms are relegated to slightly larger distances (corresponding to positions nearer the less interactive CW atoms), and the second peak increases as the first peak becomes a shoulder.

The most interesting features of the three panels in Figure 2a are revealed when one considers IL series with progressively longer alkyl chains; in all cases, the xenon atoms start to "disappear" from the vicinity of the imidazolium ring. This effect is more pronounced in the case of the chloride-based ILs and less distinct in the case of the $[Ntf_2]^-$-based ILs. Obviously, the xenon atoms prefer to dissolve in the progressively larger nonpolar regions, and the driving force for such a "migration" is larger in the chloride-based ILs.

This trend can be further appreciated if one takes into account Figure 2b, which shows the intensity of the first peak of the RDFs between the xenon atoms and the terminal atoms of the alkyl side chain. Even for $[C_2mim]$-based ILs, the intensity of the first Xe-CT peak is already larger than those corresponding to the Xe-CR RDFs (the xenon atoms tend to concentrate in the vicinity of the small clusters of lower charge density areas formed by the ethyl moieties of the cation). In this case, the anion effect is rather small, especially taking into account the estimated statistical error associated with the determination of the intensities (depicted in Figure 2b for the $[C_nmim]Cl$ RDFs). However, for larger n values, the intensities of the Xe-CT RDF first peaks become larger, reaching maxima around 3 for the $[C_{10}mim]$-based ILs. This trend seems to indicate that as larger nonpolar domains become available, the xenon will start to concentrate more in those regions and farther away from the polar network. The results in Figure 2a and b also suggest that this xenon concentration gradient is steepest for the chloride-based ILs, followed by $[PF_6]^-$- and $[Ntf_2]^-$-based ones.

The distribution of xenon atoms along the alkyl side chains of $[C_{10}mim]$-based ILs is shown in the three panels of Figure 2c. When one considers the other carbon atoms of the decyl chain, one can see a completely regular trend decreasing from C9 to C1. Again, the trend is stronger for the $[C_{10}mim]Cl$, followed by $[C_{10}mim][PF_6]$ and $[C_{10}mim][Ntf_2]$. The xenon

dx.doi.org/10.1021/jz401279u | J. Phys. Chem. Lett. 2013, 4, 2758−2762

distribution is in fact quite subtle; not only does it tend to move away from the polar regions, but it does so in a gradual way that depends on the nature of the anion. Such insights via MD modeling suggest that xenon can indeed be used as a very effective probe for the study of ILs as complex, nanostructured fluids.

As an example, Figure 3 shows the $[C_n\text{mim}][\text{Ntf}_2]$ $\delta\text{Xe}(n)$ data on an expanded scale, where a clear change in the slope is

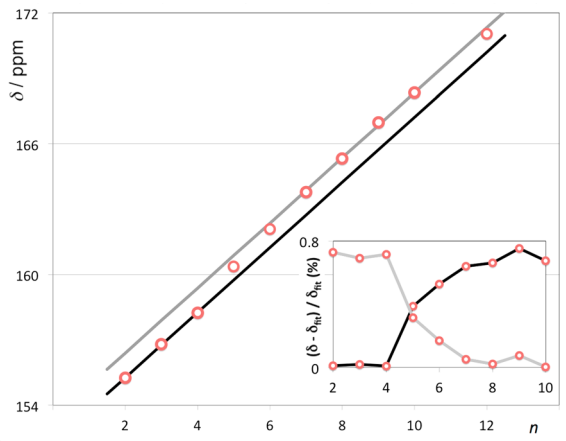

Figure 3. ^{129}Xe chemical shifts, δ, as a function of the alkyl chain length, n, in $[C_n\text{mim}][\text{Ntf}_2]$. The inset shows the relative deviations (%) from the black and gray fits along the series.

seen at around $n = 5$. This behavior is perfectly consistent with several proposals[1,5] of a change in the liquid structure in this series at around $n = 5$, from a media with dispersed nonpolar small clusters to a bicontinuous structure formed by a polar network permeated by an uninterrupted nonpolar domain. The upward displacement of δXe at $n = 5$ (to values closer to those characteristic of alkanes) is compatible with the percolation of the nonpolar region, allowing the xenon to probe more effectively the alkyl domains.

In conclusion, the results show that xenon is able to clearly distinguish between different families of ILs (including different types of interaction with different types of anion/polar networks) and, more importantly, to provide information on how the complex structure of an IL evolves along a homologous series. Further studies using ^{129}Xe as a unique and distinctive probe are indeed warranted in the context of ILs studies.

■ ASSOCIATED CONTENT

Supporting Information

Materials, sample preparation, ^{129}Xe NMR procedures and data, simulation methodology, and RDF values. This material is available free of charge via the Internet at http://pubs.acs.org.

■ AUTHOR INFORMATION

Corresponding Author

*E-mail: jnlopes@ist.utl.pt (J.N.C.L); efilipe@ist.utl.pt (E.J.M.F.).

Notes

The authors declare no competing financial interest.

■ ACKNOWLEDGMENTS

Financial support was provided by Fundação para a Ciência e Tecnologia (FCT) through Projects PTDC/CTM-NAN/121274/2010, FCT-ANR/CTM-NAN/0135/2012, Pest-OE/QUI/UI0100/2013, and Pest-OE/EQB/LA0004/2011. The National NMR Network (REDE/1517/RMN/2005) was supported by POCI 2010 and FCT. P.M., and K.S. acknowledge Postdoc Grants SFRH/BPD/81748/2011 and SFRH/BPD/38339/2007 also from FCT.

■ REFERENCES

(1) Triolo, A.; Russina, O.; Bleif, H. J.; Di Cola, E. Nanoscale Segregation in Room Temperature Ionic Liquids. *J. Phys. Chem. B* **2007**, *111*, 4641−4644.

(2) Wang, J.; Voth, G. A. Unique Spatial Heterogeneity in Ionic Liquids. *J. Am. Chem. Soc.* **2005**, *127*, 12192−12193.

(3) Canongia Lopes, J. N.; Pádua, A. A. H. Nanostructural Organization in Ionic Liquids. *J. Phys. Chem. B* **2006**, *110*, 3330−3335.

(4) Tokuda, H.; Hayamizu, K.; Ishii, K.; Susan, M. A. B. H.; Watanabe, M. Physicochemical Properties and Structures of Room Temperature Ionic Liquids. 2. Variation of Alkyl Chain Length in Imidazolium Cation. *J. Phys. Chem. B* **2005**, *109*, 6103−6110.

(5) Rocha, M. A. A.; Lima, C. F. R. A. C.; Gomes, L. R.; Schröder, B.; Coutinho, J. A. P.; Marrucho, I. M.; Esperança, J. M. S. S.; Rebelo, L. P. N.; Shimizu, K.; Canongia Lopes, J. N.; Santos, L. M. N. B. F. High-Accuracy Vapor Pressure Data of the Extended $[C_nC_1\text{im}][\text{Ntf}_2]$ Ionic Liquid Series: Trend Changes and Structural Shifts. *J. Phys. Chem. B* **2011**, *115*, 10919−10926.

(6) Macchiagodena, M.; Gontrani, L.; Ramondo, F.; Triolo, A.; Caminiti, R. Liquid Structure of 1-Alkyl-3-methylimidazolium-hexafluorophosphates by Wide Angle X-ray and Neutron Scattering and Molecular Dynamics. *J. Chem. Phys.* **2011**, *134*, 114521.

(7) Macchiagodena, M.; Ramondo, F.; Triolo, A.; Gontrani, L.; Caminiti, R. Liquid Structure of 1-Ethyl-3-methylimidazolium Alkyl Sulfates by X-ray Scattering and Molecular Dynamics. *J. Phys. Chem. B* **2012**, *116*, 13448−13458.

(8) Bowron, D. T.; D'Agostino, C.; Gladden, L. F.; Hardacre, C.; Holbrey, J. D.; Lagunas, M. C.; McGregor, J.; Mantle, M. D.; Mullan, C. L.; Youngs, T. G. A. Structure and Dynamics of 1-Ethyl-3-methylimidazolium Acetate via Molecular Dynamics and Neutron Diffraction. *J. Phys. Chem. B* **2010**, *114*, 7760−7768.

(9) Hardacre, C.; Holbrey, J. D.; Mullan, C. L.; Youngs, T. G. A.; Bowron, D. T. Small Angle Neutron Scattering from 1-Alkyl-3-methylimidazolium Hexafluorophosphate Ionic Liquids ($[C_n\text{mim}][\text{PF}_6]$, $n = 4$, 6, and 8). *J. Chem. Phys.* **2010**, *133*, 074510.

(10) Xiao, D.; Rajian, J. R.; Cady, A.; Li, S.; Bartsch, R. A.; Quitevis, E. L. Nanostructural Organization and Anion Effects on the Temperature Dependence of the Optical Kerr Effect Spectra of Ionic Liquids. *J. Phys. Chem. B* **2007**, *111*, 4669−4677.

(11) Xiao, D.; Rajian, J. R.; Hines, L. G.; Li, S.; Bartsch, R. A.; Quitevis, E. L. Nanostructural Organization and Anion Effects in the Optical Kerr Effect Spectra of Binary Ionic Liquid Mixtures. *J. Phys. Chem. B* **2008**, *112*, 13316−13325.

(12) Coleman, S.; Byrne, R.; Minkovska, S.; Diamond, D. Investigating Nanostructuring within Imidazolium Ionic Liquids: A Thermodynamic Study Using Photochromic Molecular Probes. *J. Phys. Chem. B* **2009**, *113*, 15589−15596.

(13) Mele, A.; Romano, G.; Giannone, M.; Ragg, E.; Fronza, G.; Raos, G.; Marcon, V. The Local Structure of Ionic Liquids: Cation−Cation NOE Interactions and Internuclear Distances in Neat $[\text{BMIM}][\text{BF}_4]$ and $[\text{BDMIM}][\text{BF}_4]$. *Angew. Chem., Int. Ed.* **2006**, *45*, 1123−1126.

(14) Gutel, T.; Santini, C. C.; Pádua, A. A. H.; Fenet, B.; Chauvin, Y.; Canongia Lopes, J. N.; Bayard, F.; Costa Gomes, M. F.; Pensado, A. S. Interaction Between the π-System of Toluene and the Imidazolium Ring of Ionic Liquids: A Combined NMR and Molecular Simulation Study. *J. Phys. Chem. B* **2009**, *113*, 170−177.

(15) Puttick, S.; Davis, A. L.; Butler, K.; Lambert, L.; El Harfi, J.; Irvine, D. J.; Whittaker, A. K.; Thurecht, K. J.; Licence, P. NMR as a Probe of Nanostructured Domains in Ionic Liquids: Does Domain

Segregation Explain Increased Performance of Free Radical Polymerisation? *Chem. Sci.* **2011**, *2*, 1810−1816.
(16) Fumino, K.; Wittler, K.; Ludwig, R. The Anion Dependence of the Interaction Strength Between Ions in Imidazolium-Based Ionic Liquids Probed by Far-Infrared Spectroscopy. *J. Phys. Chem. B* **2012**, *116*, 9507−9511.
(17) Puttick, S.; Davis, A. L.; Butler, K.; Irvine, D. J.; Licence, P.; Thurecht, K. J. The Influence of Domain Segregation in Ionic Liquids Upon Controlled Polymerisation Mechanisms: RAFT Polymerisation. *Polym. Chem.* **2013**, *4*, 1337−1344.
(18) Mandal, P. K.; Sarkar, M.; Samanta, A. Excitation-Wavelength-Dependent Fluorescence Behavior of Some Dipolar Molecules in Room-Temperature Ionic Liquids. *J. Phys. Chem. A* **2004**, *108*, 9048−9053.
(19) Crowhurst, L.; Mawdsley, P. R.; Perez-Arlandis, J. M.; Salter, P. A.; Welton, T. Solvent-Solute Interactions in Ionic Liquids. *Phys. Chem. Chem. Phys.* **2003**, *5*, 2790−2794.
(20) Reisse, J. Monoatomic Xenon — Its Great Interest in Chemistry as a Probe of Intermolecular Interactions, and Its (Easy) Study by NMR. *New J. Chem.* **1986**, *10*, 665−672.
(21) Dybowski, C.; Bansal, N.; Duncan, T. M. NMR-Spectroscopy in Confined Spaces — Clathrates, Intercalates, and Zeolites. *Annu. Rev. Phys. Chem.* **1991**, *42*, 433−464.
(22) Jokisaari, J. NMR of Noble-Gases Dissolved in Isotropic and Anisotropic Liquids. *Prog. Nucl. Magn. Reson. Spectrosc.* **1994**, *26*, 1−26.
(23) Blakey, I.; Thurecht, K. J.; Whittaker, A. K. High-Pressure Real-Time ^{129}Xe NMR: Monitoring of Surfactant Conformation During the Self-Assembly of Reverse Micelles in Supercritical Carbon Dioxide. *Chem. Commun.* **2010**, *46*, 2850−2852.
(24) Varcoe, K. M.; Blakey, I.; Chirila, T. V.; Hill, A. J.; Whittaker, A. K. The Effect of Synthetic Conditions on the Free Volume of Poly(2-hydroxyethyl methacrylate) as Studied by (1)H NMR, ^{129}Xe NMR, and Position Annihilation Spectroscopy. *ACS Symp. Ser.* **2007**, *963*, 391−409.
(25) Oros, A.-M.; Shah, N. J. Hyperpolarized Xenon in NMR and MRI. *Phys. Med. Biol.* **2004**, *49*, R105−R153.
(26) Gerken, M.; Schrobilgen, G. J. The Impact of Multi-NMR Spectroscopy on the Development of Noble-Gas Chemistry. *Coord. Chem. Rev.* **2000**, *197*, 335−395.
(27) Filipe, E. J. M.; Dias, L. M. B.; Calado, J. C. G.; McCabe, C.; Jackson, G. Is Xenon an "Ennobled" Alkane? *Phys. Chem. Chem. Phys.* **2002**, *4*, 1618−1621.
(28) Morgado, P.; Bonifácio, R.; Martins, L. F. G.; Filipe, E. J. M. Probing the Structure of Liquids with ^{129}Xe NMR Spectroscopy: *n*-Alkanes, Cycloalkanes and Branched Alkanes. *J. Phys. Chem. B* **2013**, *117*, 9014−9024.
(29) Castiglione, F.; Simonutti, R.; Mauri, M.; Mele, A. Cage-Like Local Structure of Ionic Liquids Revealed by a ^{129}Xe Chemical Shift. *J. Phys. Chem. Lett.* **2013**, *4*, 1608−1612.
(30) Kumełan, J.; Pérez-Salado Kamps, A.; Tuma, D.; Maurer, G. Solubility of the Single Gases Methane and Xenon in the Ionic Liquid [hmim][Tf_2N]. *Ind. Eng. Chem. Res.* **2007**, *46*, 8236−8240.
(31) Rebelo, L. P. N.; Canongia Lopes, J. N.; Esperança, J. M. S. S.; Filipe, E. J. M. On the Critical Temperature, Normal Boiling Point, and Vapor Pressure of Ionic Liquids. *J. Phys. Chem. B* **2005**, *109*, 6040−6043.
(32) Lim, Y. H.; Calhoun, A. R.; King, A. D. NMR Chemical Shifts of ^{129}Xe Dissolved in Liquid Haloalkanes and Their Mixtures. *Appl. Magn. Reson.* **1997**, *12*, 555−574.